*Key Engineering Materials*
*ISSN: 1662-9795, Vol. 926, pp 443-451*
*doi:10.4028/p-54m016*

*Submitted: 2021-12-08*
*Revised: 2022-01-27*
*Accepted: 2022-01-28*
*Online: 2022-07-22*

# Towards Multi-Scale Modeling of Zirconium Alloys Recrystallization and Application to Thermo-Mechanical Processes Optimization

GAILLAC Alexis[1,a*], GRAND Victor[1,2,b], ARSEN Alan[1,c], GAILLARD Quentin[1,d] and BERNACKI Marc[2,e]

[1]Framatome Ugine, CRC, Avenue Paul Girod, CS 90100, 73403 Ugine, France

[2]Cemef – Mines Paristech, 1 rue Claude Daunesse, CS 10207, 06904 Sophia Antipolis, France

[a]alexis.gaillac@framatome.com, [b]victor.grand@mines-paristech.fr, [c]alan.arsen@gmail.com, [d]quentingaillard30@hotmail.fr, [e]marc.bernacki@mines-paristech.fr

**Keywords:** zirconium, recrystallization, modeling, extrusion.

**Abstract.** Zirconium alloys are used in the nuclear industry due to their low neutron capture cross-section and resistance to corrosion, irradiation and creep. The microstructure of the nuclear fuel components evolves during the manufacturing route and can impact the subsequent processes or the final properties. Thus, numerical modeling of thermo-mechanical manufacturing processes is of interest to understand and master these microstructure evolutions.

Numerical modeling of thermo-mechanical manufacturing processes with FORGE® NxT[1] software is applied. These models provide the thermo-mechanical history of the material at each integration point of the finite element (FE) mesh, which can be used to assess locally the continuous dynamic and post-dynamic recrystallization during hot extrusion.

Mean-field models were developed in Python and integrated into FORGE® NxT software, to quantify the microstructure evolution at the macro-scale of the component. Full-field models (DIGIMU® software[1]) were also developed for considering microstructural heterogeneities and the influence of initial microstructure at the mesoscopic scale while improving the mean-field equations by homogenization.

After validation based on experimental results, these two recrystallization models provide complementary information to optimize the process parameters at the macro-scale and to better understand mesoscopic scale phenomena, such as:

- At the macro-scale: influence of hot extrusion parameters on the continuous dynamic and post-dynamic recrystallization of Zircaloy-4
- At the meso-scale: influence of the initial microstructure on the recrystallization phenomena with improved precision. Indeed, the topology of the microstructure is predicted and not only the mean values/distributions of the state variables.

## Introduction

Zirconium alloys are used in the nuclear fuel assemblies due to their low neutron capture cross-section and resistance to corrosion, irradiation and creep within the BWR (Boiling Water Reactor) or PWR (Pressurized Water Reactor) environment [1]. The forming route of zirconium alloys cladding tubes includes the following main processes [2]:

- Ingots VAR melting and remelting
- Open-die hot forging of ingots into forged bars
- Beta-quenching of forged bars and machining of billets
- Hot extrusion of billets into tube hollows
- Several cold rolling passes and intermediate heat treatments
- Final heat treatment of tubes

[1] FORGE and DIGIMU are registered trademarks of TRANSVALOR S.A.

Cladding tubes integrity must be ensured during the whole life of the fuel assembly to confine the nuclear fuel and the fission products. Reliability of the cladding tubes is ensured by a 100% quality control of the manufactured tubes. This quality is given by the final geometry, surface roughness and microstructure, which is inherited from the whole manufacturing route. Thus, the thermo-mechanical processes and associated microstructures evolutions must be mastered and optimized to get the right properties of the final tubes. For this purpose, numerical models of thermo-mechanical processes, including microstructure evolution models, were established [3]. The aim of this paper is to present the on-going developments of these models and the associated characterizations, focusing on the example of tubes hot extrusion process.

For zirconium alloys, the following recrystallization mechanisms are reported in the literature and will be discussed: During hot forming processes of zirconium alloys, continuous dynamic recrystallization (CDRX) occurs, and the microstructure evolves by a progressive development of sub-grains (LAGB: low angle grain boundaries) which transform into new grains (HAGB: high angle grain boundaries) as the strain increases [4]. This mechanism interacts with recovery which is also active at high temperature. In this paper, only the case of monophasic alloy processing (meaning α-Zr phase + second phase particles, without β-Zr phase) is considered, which is consistent with the hot extrusion of zircaloy-4 alloy.

Following hot forming processes, post-dynamic recrystallization (PDRX) occurs during the cooling of the part or during a subsequent heat-treatment. The new grains and sub-grains formed during the hot deformation grow at the expense of deformed ones. If the heat treatment is long enough, pure grain growth in fully recrystallized zones can also take place [5, 6]. Compared to SRX, new grains and sub-grains were previously developed during CDRX and no grain nucleation is assumed to occur in this PDRX stage.

Finally, during heat treatments following cold forming processes, static recrystallization (SRX) occurs, and the microstructure evolves by nucleation of new grains and their growth at the expense of deformed ones [6]. If the heat treatment is long enough, pure grain growth can also become the dominant mechanism [5]. Static recrystallization differs from post-dynamic one by the initial microstructure, which does not include sub-grains in the case of a cold forming process. This type of recrystallization can also be modeled using mean-field and full-field models, but this is out of the scope of this paper which will focus on hot forming processes.

## Recrystallization Characterization

**Methods.** Recrystallization was characterized on zircaloy-4 industrial samples after hot extrusion and laboratory compression tests with additional heat treatments. Both type of samples were prepared with a final electro-polishing, and an EBSD analysis was performed and post-processed using Matlab and the MTEX toolbox. Extrusion samples were also analyzed with optical microscopy to assess the recrystallized fraction based on the fraction of equiaxed grains.

**Industrial samples.** Tubes were extruded with the industrial standard extrusion parameters which are an extrusion ratio of about 10 and an initial temperature of 600°C .Mode details about this hot extrusion process and associated parameters can be found in [9]. Microstructure was characterized at mid-thickness, at 4 different positions from the front end of an extruded tube (0, 60, 150 and 300 mm) with optical microscopy, and at 2 positions (60 and 300 mm) with EBSD. Fig. 1 and Fig. 2 shows respectively optical micrographs and EBSD KAM maps (Kernel Average Misorientation) at the same positions. In both figures, horizontal axis is the longitudinal direction and vertical axis is the radial direction of the tube. Recrystallized fraction can be first estimated from optical micrographs, assuming that equiaxed grains are recrystallized ones. A more accurate recrystallization fraction can be measured from EBSD orientation map, with a criterion based on GAKAM < 0,4° (Grain Average Kernel Average Misorientation) or GAKAM < 0,4° and GOS < 3° (Grain Orientation Spread). Fig. 3 summarizes the results of different criteria for optical micrographs and EBSD. Even if the microstructure is not homogeneous at a given position, the recrystallized fraction clearly increases after the front end of the tube and a steady state seems to be reached after 150 mm of extrusion. The decrease of recrystallization fraction observed between 150mm and 300mm is not considered to be

significant because of the scatter in microstructure that was observed in the samples but not precisely quantified. The GAKAM criteria is consistent with the fraction of recrystallized grains assumed as equiaxed ones on the optical micrographs. The GAKAM + GOS criteria gives a lower recrystallized fraction at 150 mm. This is due to the presence of sub-grains with a misorientation greater than 3° in some big grains, which fulfill the GAKAM criteria but not the GOS one. Defining a recrystallization criterion from EBSD data is then not obvious for CDRX and PDRX due to the presence of the sub-structure.

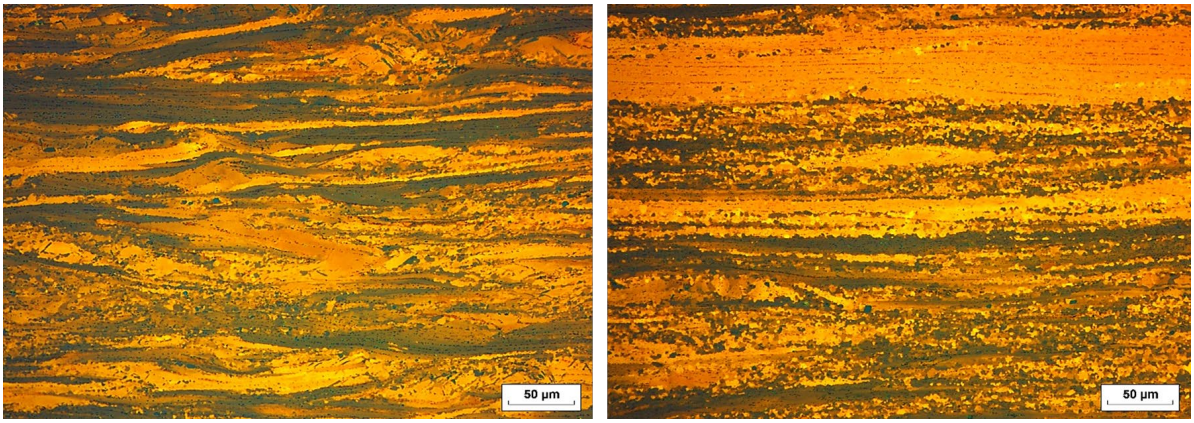


Fig. 1: Microstructure by optical microscopy, at mid-thickness of a zircaloy-4 extruded tube, at 60 mm (left) and 300 mm (right) from the front end of the tube.

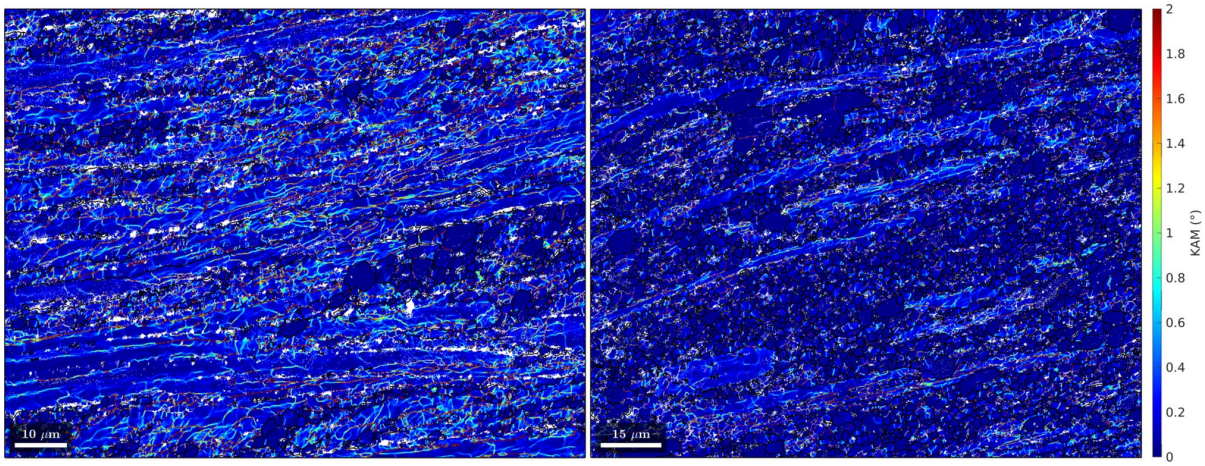


Fig. 2: EBSD KAM maps, at mid-thickness of a zircaloy-4 extruded tube, at 60 mm (left) and 300 mm (right) from the front end of the tube.

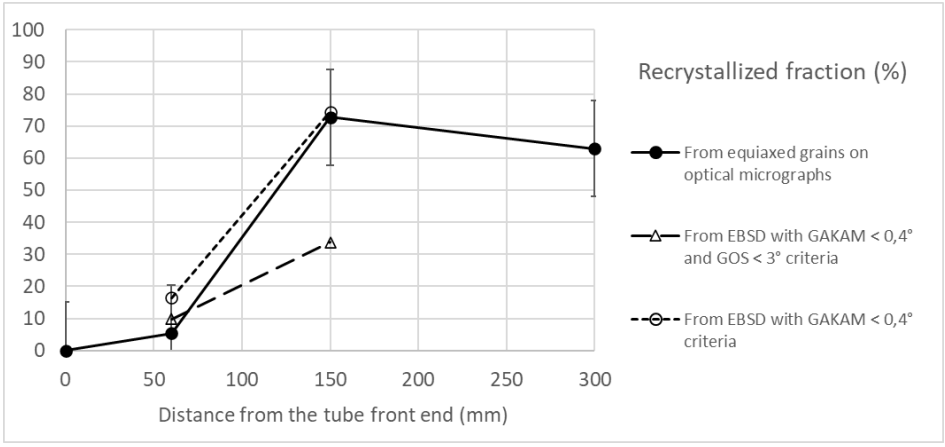


Fig. 3: Recrystallized fraction at mid thickness of a zircaloy-4 extruded tube, at different positions from the front end of an extruded tube, from optical micrographs and EBSD.

**Laboratory samples.** To identify the recrystallization models parameters in better controlled conditions compared to industrial processes, zircaloy-4 samples were characterized by EBSD after laboratory compression tests and heat-treatments. A full compression test matrix was performed with three temperatures (450°C / 550°C / 650°C), three strain levels (0,65 / 1 / 1,35) and three strain rates ($0{,}01s^{-1}$ / $0{,}1s^{-1}$ / $1s^{-1}$). Moreover, additional heat treatments were applied to selected samples. These experiments give a good overview of microstructures after CDRX and PDRX in representative thermo-mechanical conditions compared to industrial hot extrusion process. Fig. 4 illustrates an example of microstructure evolution during the heat treatment at 650°C after a compression test at the same temperature, a strain of 1,35 and a strain rate of $1s^{-1}$. A fast evolution of the microstructure by PDRX mechanisms can be seen, pointing out the importance of thermal conditions occurring just after hot deformation. The full test matrix, that is still under post-processing, will be a valuable basis for the identification of mean field and full-field model parameters.

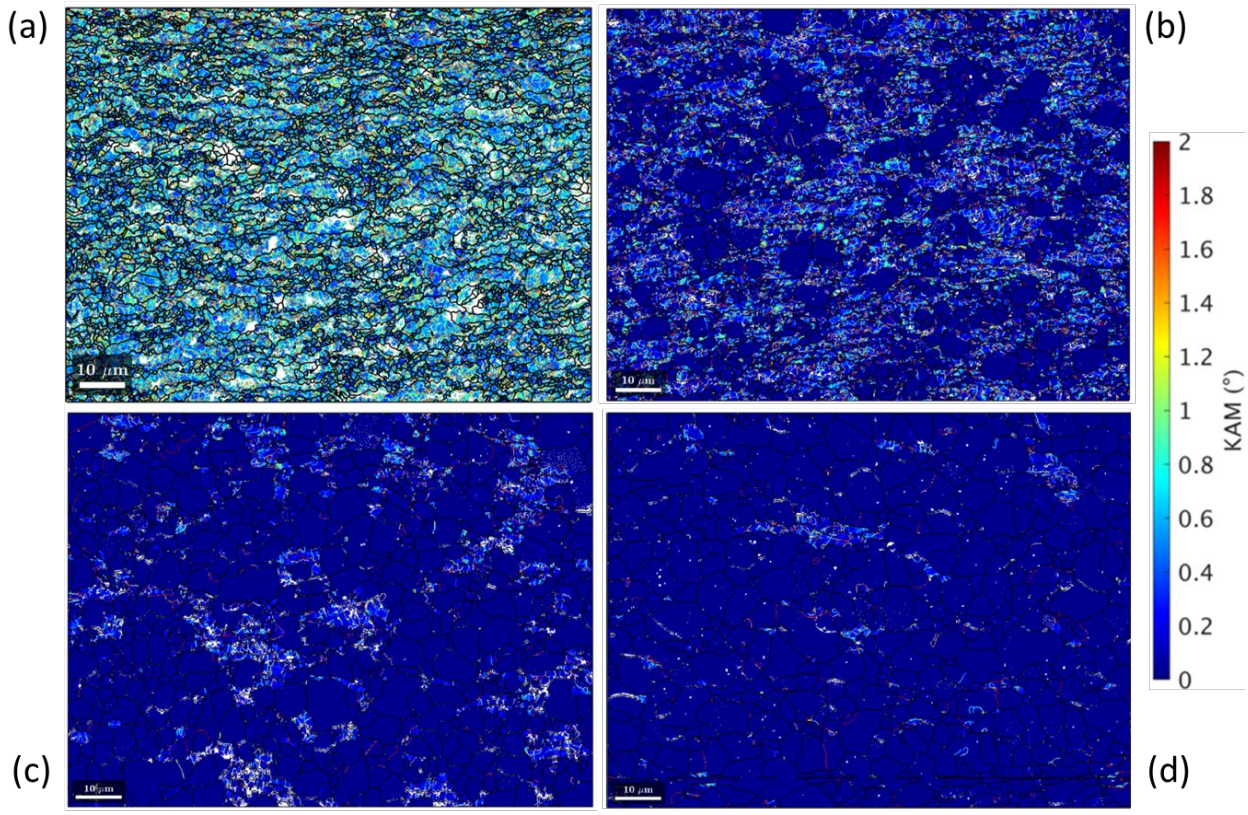


Fig. 4: EBSD KAM maps on zircaloy-4 samples after compression (temperature 650°C, strain 1,35, strain rate 1s-1) and subsequent heat treatments at 650°C for 1s (a), 50s (b), 100s (c) and 200s (d).

## Recrystallization Modeling

**Modeling of the whole manufacturing route.** Since the 1990s, Framatome has developed the numerical modeling of the zirconium alloys manufacturing processes, including VAR melting [7], forming [3, 8, 9], heat treatments and assembly processes [10] to better understand and master these processes or to lower the cost and potential risk for new developments.

**Hot extrusion of tubes.** Together with laboratory tests and experimental characterizations, numerical modeling of extrusion process gives compulsory data for the understanding and modeling of microstructure evolutions during this process. Indeed, microstructure evolution is a function of the thermo-mechanical history of the material, namely strain, strain rate and temperature during extrusion (dynamic recrystallization) and during the cooling of the tube or further heat-treatment (post-dynamic recrystallization). The finite element model developed with FORGE® NxT software and presented in detail in [9] can provide such data, as the one presented in Fig. 5. A sharp increase of strain and strain rate can be observed during the deformation of the tube in the conical die (between 15s and 24,5s), together with an increase of temperature as a consequence of the dissipated plastic power.

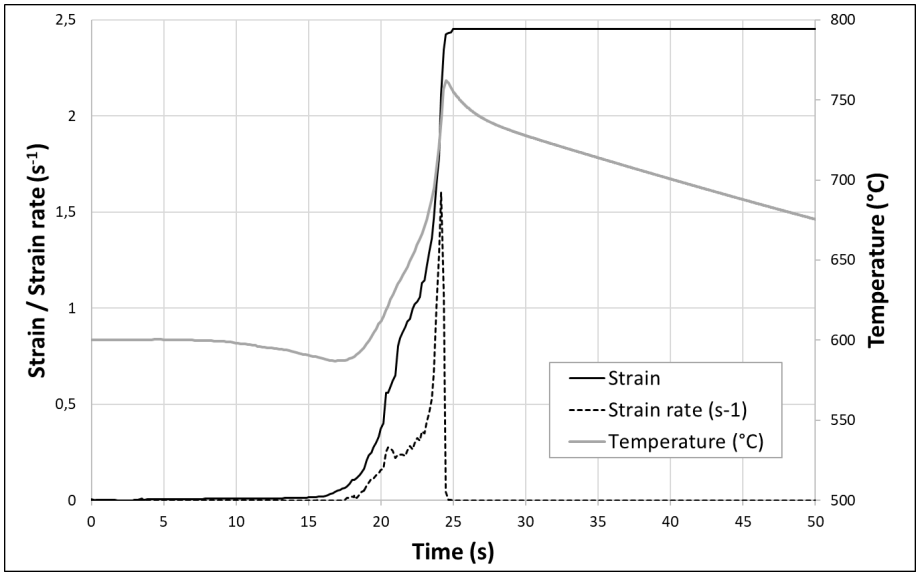


Fig. 5: Thermo-mechanical history of the material during (between 15s and 24,5s) and after extrusion (after 24,5s), from FE model, at mid-thickness of a zircaloy-4 tube and at extrusion steady-state.

**Recrystallization mean-field model.** The recrystallization mean-field model is based on the Gourdet-Montheillet model [11], initially developed for aluminum alloys and further adapted by Gaudout [12] for application to zirconium alloys α-phase recrystallization. It includes a CDRX model and a PDRX one. The CDRX model describes the recovery and the fragmentation of the microstructure during extrusion, as a consequence of the progressive development of sub-grains which transforms into new grains as the strain and dislocation density increase (Fig. 6). The PDRX model is based on Avrami approach [13] and describes the growth of recrystallized grains during the cooling of the extruded tube or subsequent heat treatment. The mean-field model equations are described in detail in [12]. The latest version of the model is coded on Python with a graphical user interface. It is also coded on FORGE® NxT software as a user variable. It is used to assess the evolution of the microstructure (recrystallized fraction, grain size, LAGB density, dislocation density) as a function of the local thermo-mechanical history of the material during and after hot forming.

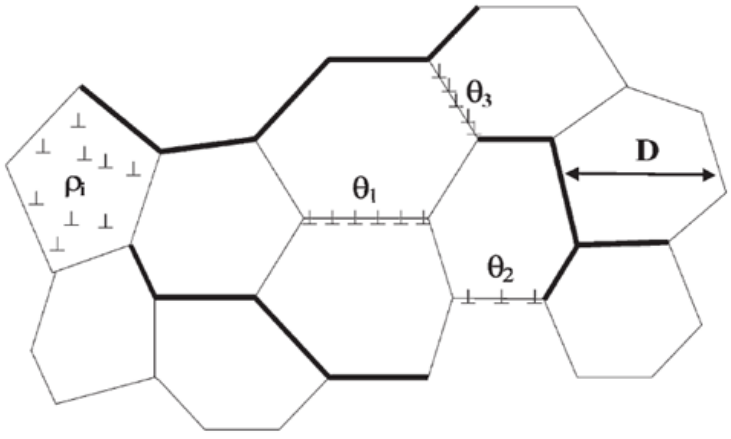


Fig. 6: Schematic representation of the microstructure during fragmentation [11]. Thick lines are HAGB (crystallographic misorientation > 15°), fine lines are LAGB (<15°).

**Recrystallization full-field model.** The recrystallization full-field model is based on a level set description of interfaces (grain boundaries and second phase particles) in a FE framework. It was first developed by Bernacki et al. [14] and followed by many improvements. The baseline model (DIGIMU® software) used in this study includes the Smith-Zener pinning effect (pining of grain boundaries by second phase particles [15]) and the influence of stored energy in the form of dislocation density [16], as well as the latest computational performance improvements [17] that allows 2D and 3D computations including the main physics of dynamic and post-dynamic

recrystallization [18]. The equations of this model are described in detail in these references [14, 16, 17, 18].

The baseline full-field model includes the discontinuous dynamic recrystallization mechanisms, characterized by the nucleation of new grains based on a critical strain criterion [18]. The continuous ones, characterized by the progressive nucleation and misorientation of the sub-grains and occurring in zirconium alloys, are under development and will include the orientation dependence of LAGB mobility and energy (Fig. 7) [19]. These developments and corresponding equations will be presented in [19] and others upcoming references.

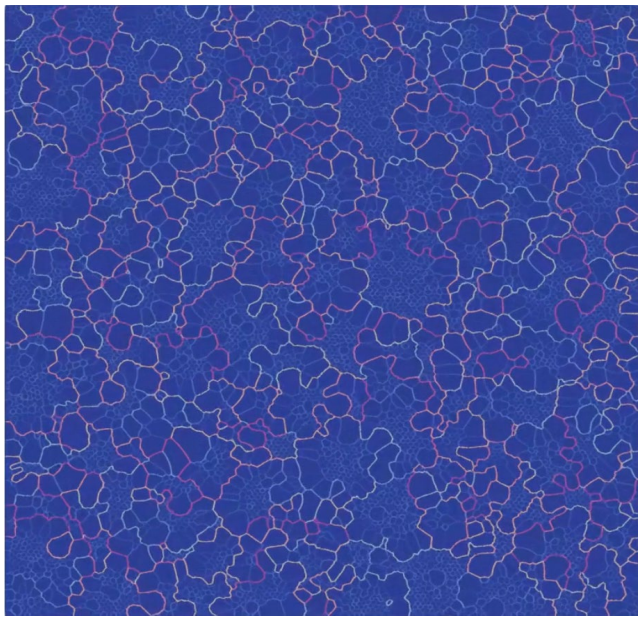

Fig. 7: Representative elementary volume of the microstructure in the 2D full field model after pure grain growth (without stored energy), including grains (HAGB, thick lines) and sub-grains (LAGB, thin lines) [19].

**Identification and validation of models parameters.** The mean-field model coded on Python was first applied as a post-processing of thermomechanical loading during compression tests that was calculated using FORGE® NxT modeling. At that time, only CDRX EBSD results (with only 1 or 2 seconds of PDRX due to the time needed to quench the samples) were available. A sensitivity analysis was performed on the 23 parameters of the model. Since most of the experiments did not exhibit significant PDRX, CDRX model parameters were identified as the more influent, except the activation energy of grain boundary mobility which can have a significant impact for some experiments with short PDRX times. A total of 7 parameters were then selected for an automated optimization using a Monte Carlo approach, aiming to reduce the difference between modeled recrystallization fraction and experimental one. By randomly testing $10^5$ to $10^6$ set of parameters, this optimization process was able to reduce the figure of merit by about 40% compared with the initial parameters defined in a previous work [12]. It is worth mentioning that the scatter of CDRX recrystallized fraction was quite large due to its relatively low value compared to the precision that can be achieved from EBSD on heavily deformed samples. This optimization process will be performed again with the whole set of compression tests results that are still on-going and will include the CDRX and PRDX parameters.

The first step for the identification of full field model parameters was the modeling of pure grain growth. In this case, without stored energy due to dislocations, meaning in a fully recrystallized material, grains growth rate is only a function of the grain boundaries energy and mobility. Assuming a grain boundary energy of 0,22 $J.m^{-2}$ from the bibliography [20], the mobility was identified by an iterative fitting of modeling compared to experimental results (see [21] for more details concerning this procedure). For this purpose, grain growth was characterized as a function of time and temperature for an alloy reproducing the behavior of zircaloy-4 without the presence of SPPs (Second

Phase Particles), i.e. same solid solution as zircaloy-4 without alloying elements forming SPPs. After this identification process for mobility (function of temperature), the experimental and modeling results are consistent (Fig. 8). In this figure, equivalent grain diameter is defined by the equivalent circle diameter having the same surface as the characterized grain.

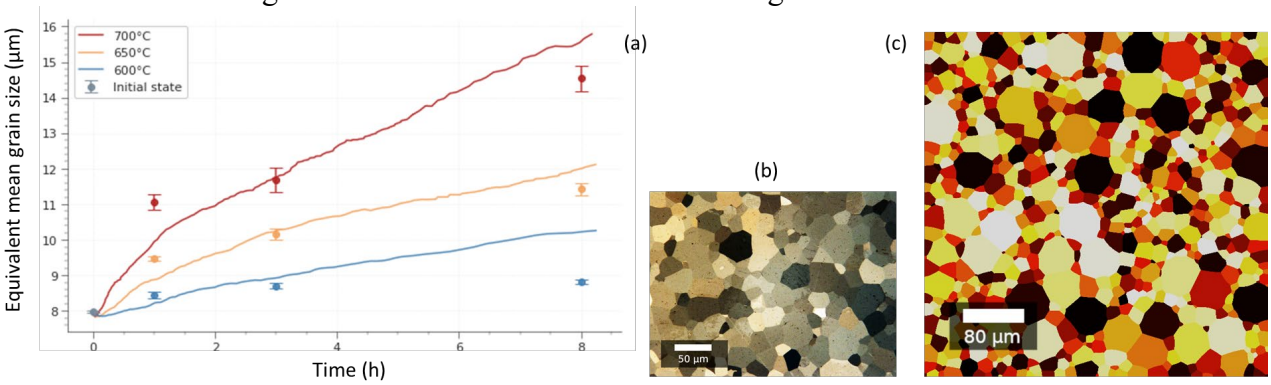


Fig. 8: Grain growth as a function of time and temperature in "zircaloy-4 without SPPs" from experiment and full-field modeling (a). Final microstructure after 8h at 700°C from experiment (b) and full-field modeling (c).

In a second step, the good behavior of the model for SPPs effect on grain growth by Smith-Zener pinning phenomenon [15] was validated by comparing experimental results and numerical ones. For this purpose, grain growth was characterized as a function of time and temperature for a commercial zircaloy-4 including SPPs. The initial microstructure, including SPPs, was introduced in the model and the previously identified grain boundaries mobility and energy was used. For lower temperatures (600°C and 650°C), the model results are consistent with experimental ones (Fig. *9*), which both reach a stable maximum grains size according to the Smith-Zener pinning phenomenon. For the higher temperature (700°C), experiments exhibit faster grain growth. It was checked that the partial dissolution of precipitates at this temperature, which is not yet considered in the model, was responsible for the reduction of the Smith-Zener pinning pressure.

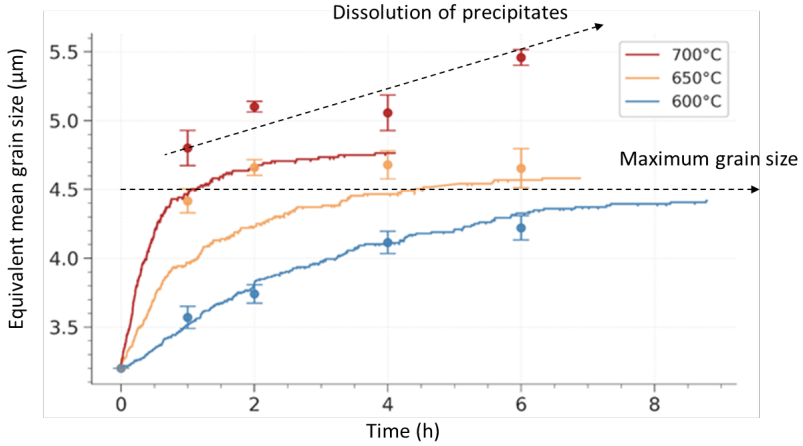


Fig. 9: Grain growth as a function of time and temperature in commercial zircaloy-4 with SPPs from experiment and full-field modeling.

The last step will be the validation of the full-field CDRX and PDRX model based on the full compression and heat treatments test matrix. This model will include the progressive nucleation and misorientation of the sub-grains and the orientation dependence of LAGB mobility and energy. It will be able to predict the complex microstructures evolutions occurring during the thermo-mechanical and heat treatments processes of interest.

## Conclusions

**Characterizations.** CDRX and PDRX of zircaloy-4 alloy were characterized by optical microscopy and EBSD on industrial extruded tubes and compression tests samples. These are a valuable data set for the understanding of recrystallization mechanisms occurring in zirconium alloys during and after hot forming processes. Nevertheless, a finer analysis of EBSD data will be needed to get reliable results for the identification of recrystallization models parameters.

**Modeling.** A physically based mean-field model was developed to describe the CDRX and PDRX mechanisms. The latest Python version of this model allowing fast computations, a Monte-Carlo approach can be used to optimize the parameters, thanks to the compression and heat treatments test results. The full-field model is still under development for CDRX and PDRX mechanisms, but it is already validated for the modeling of pure grain growth with or without SPPs.

## Perspectives

**Macro scale industrial application.** Once validated based on experimental results, the mean-field model will be used to assess the influence of hot extrusion parameters such as temperature, extrusion ratio, ram speed and cooling kinetics after extrusion. This fast model can be applied in several locations in the part, giving a full overview of the recrystallization at the macro-scale. It could also be introduced in the extrusion FE model as a user variable.

**Mesoscopic scale industrial application.** The full-field model will be able to assess mesoscopic scale phenomena such as the influence of the initial microstructure (morphology of grains, size and distribution of SPPs). Indeed, it was observed that quenched billets behave differently depending on the initial microstructure inherited from the previous processes. At constant extrusion parameters, a microstructure with a large amount of parallel alpha plates and aligned SPPs at the plates boundaries will give a lower recrystallization ratio compared to a basketweave microstructure with a more homogeneous distribution of SPPs. In both cases, the microstructure will further recrystallize during the subsequent processes, giving homogenous and targeted properties of the final products. But improving the recrystallization fraction on extruded tubes can improve the formability for the subsequent cold rolling and the global performance of the manufacturing route.

## References

[1] Z. Duan et al., Current status of materials development of nuclear fuel cladding tubes for light water reactors, Nuclear Engineering and Design 316 (2017) 131-150.

[2] A. Gaillac, Mise en forme des alliages de zirconium et de hafnium, Techniques de l'ingénieur M3190 (2018).

[3] A. Gaillac and C. Ly, Optimized Manufacture of Nuclear Fuel Cladding Tubes by FEA of Hot Extrusion and Cold Pilgering Processes, Proceedings of the 21st international ESAFORM conference on material forming: ESAFORM 2018, AIP Conference Proceedings 1960 (2018).

[4] C. Chauvy, P. Barberis and F. Montheillet, Microstructure Transformation during Warm Working of Beta Treated Lamellar Zircaloy-4 within the Upper Alpha Range, Mater. Sci. Eng. A, 431 (2006) 59–67.

[5] N. Bozzolo and al., Grain Growth Texture Evolution in Zirconium (Zr702) and Commercially Pure Titanium (T40), Materials Science Forums Vols. 467-470 (2004) 441-446.

[6] M. Maric and al., How do metals with a hexagonal crystal structure recrystallise ?, submitted to Acta Materialia (2021).

[7] A. Jardy et al., Segregation in Vacuum Arc Remelted Zirconium Alloy Ingots, Zirconium in the Nuclear Industry: 16th International Symposium, ASTM STP1529 (2011), 219–243.

[8] B. Lodej, Accelerated 3D FEM Computation of the Mechanical History of the Metal Deformation in Cold Pilgering of Tubes, J. Mater. Process. Technol., Vol. 177, Nos. 1–3 (2006), 188–191.

[9] A. Gaillac et al., Numerical Modeling of Zirconium Alloys Hot Extrusion, Zirconium in the Nuclear Industry: 18th International Symposium, ASTM STP 1597 (2017), 127-150.

[10] A. Gaillac et al., Numerical Modeling of Fuel Rod Resistance Butt Welding, Zirconium in the Nuclear Industry:17th International Symposium, ASTM STP 1543 (2014), 331–345.

[11] S. Gourdet and F. Montheillet, A model of continuous dynamic recrystallization, Acta Materiala, Volume 51, Issue 9 (2003), 2685-2699.

[12] B. Gaudout et al., Modelling Dynamic and Post-Dynamic Recrystallization of Zy-4 During and After Hot Extrusion, Steel Research International 1-2 (2008), 216–223.

[13] M. Avrami, Kinetics of Phase Change. I. General Theory. The Journal of Chemical Physics, Vol. 7, No. 12 (1939), 1103–1112.

[14] M. Bernacki et al., Level set framework for the finite-element modelling of recrystallization and grain growth in polycrystalline materials, Scripta Materialia 64 (2011), 525-528.

[15] C.S. Smith, Introduction to Grains, Phases, and Interfaces, an Interpretation of Microstructure, Trans. Metall. Soc. AIME 175 (1948), 15–51.

[16] A. Agnoli et al., Development of a level set methodology to simulate grain growth in the presence of real secondary phase particles and stored energy - Application to a nickel-base superalloy, Computational Materials Science 89 (2014), 233-241.

[17] B. Scholtes et al., New finite element developments for the full field modeling of microstructural evolutions using the level-set method, Computational Materials Science 109 (2015), 388-398.

[18] L. Maire et al., Modeling of dynamic and post-dynamic recrystallization by coupling a full field approach to phenomenological laws, Materials & Design 133 (2017), 498-519.

[19] V. Grand et al., Characterization and modeling of the influence of initial microstructure on recrystallization of zircaloy-4 during hot forming. In 20$^{th}$ International Symposium on Zirconium in the Nuclear Industry, Ottawa, Canada, June 20–23 2022.

[20] J.W.C. Dunlop et al., Modelling isothermal and non-isothermal recrystallisation kinetics: Application to Zircaloy-4, Journal of Nuclear Materials 366 (2007), 178–186.

[21] K. Alvarado et al., Dissolution of the Primary γ′ Precipitates and Grain Growth during Solution Treatment of Three Nickel Base Superalloys, Metals 11(12) (2021), 1921.